Journal of Marine Science and Technology

Volume 25 | Issue 6 Article 18

EXPERIMENTAL STUDY OF DYNAMIC STABILITY OF UNDERWATER VEHICLE-MANIPULATOR SYSTEM USING ZERO MOMENT POINT

Jin-Il Kang
Ocean Science and Technology School, KIOST-KMOU, Busan, South Korea.

Hyeung-Sik Choi
Department of Mechanical Engineering, Korea Maritime and Ocean University, South Korea., hchoi@kmou.ac.kr

Mai The Vu
Ocean Science and Technology School, KIOST-KMOU, Busan, South Korea.

Nguyen Ngoc Duc
Department of Mechanical Engineering, Korea Maritime and Ocean University, South Korea.

Dae-Hyeong Ji
Department of Mechanical Engineering, Korea Maritime and Ocean University, South Korea.

See next page for additional authors

EXPERIMENTAL STUDY OF DYNAMIC STABILITY OF UNDERWATER VEHICLE-MANIPULATOR SYSTEM USING ZERO MOMENT POINT

Acknowledgements

This research is a part of the project National Research Foundation of Korea (NRF 2016R1A2B4011875) and supported by Basic Science Research Program through the National Research Foundation of Korea (NRF) funded by the Ministry of Education (2015R1D1A3A01015804).

Authors

Jin-Il Kang, Hyeung-Sik Choi, Mai The Vu, Nguyen Ngoc Duc, Dae-Hyeong Ji, and Joon-Young Kim

Journal of Marine Science and Technology, Vol. 25, No. 6, pp. 767-774 (2017)
DOI: 10.6119/JMST-017-1226-18

EXPERIMENTAL STUDY OF DYNAMIC STABILITY OF UNDERWATER VEHICLE-MANIPULATOR SYSTEM USING ZERO MOMENT POINT

Jin-Il Kang[1], Hyeung-Sik Choi[2], Mai The Vu[1],
Nguyen Ngoc Duc[2], Dae-Hyeong Ji[2], and Joon-Young Kim[2]

Key words: underwater vehicle-manipulator system, zero moment point, redundancy resolution, dynamic stability.

ABSTRACT

For manipulative underwater operations, an underwater vehicle-manipulator system (UVMS) has more degrees of freedom than those required to conduct a given mission. To follow the desired end-effector position and velocity accurately, UVMS should be able to generate trajectories of manipulators and the underwater vehicle can maintain dynamic stability of the entire system. In this paper, redundancy resolution is performed to find a solution satisfying the given task among many joint-space solutions. Also, to improve the dynamic stability of the UVMS, zero moment point (ZMP) is adopted such that it requires some constraints. For application of UVMS, a joint limitation is also taken as constraints for UVMS motion. The optimal solution for constraints is obtained through gradient projection method (GPM). To demonstrate the proposed redundancy resolution including ZMP, the UVMS composed of redundant manipulator is developed and tested. Test results show that the end-effector of the manipulator not only keeps track of the desired trajectory but also improves the stability of the UVMS.

I. INTRODUCTION

To accomplish various underwater tasks, an unmanned underwater vehicle (UUV) is equipped with underwater manipulators, which usually include appropriate end-effector. This whole system is called an underwater vehicle-manipulator system (UVMS). If the UVMS picks up or moves objects, the mass and moment of inertia of the entire system will be changed. Moreover, the motion of the manipulator affects the posture and position of the underwater vehicle and this acts as a disturbance that breaks the dynamic stability of the UVMS. For this reason, it is essential to find useful algorithms to stabilize UVMS as well as to study dynamic modeling of UVMS.

If the underwater vehicle of the UVMS is a hovering type with a number of degrees of freedom (DOF), the UVMS has redundancy. This extra DOFs can be used to generate a self-motion that can fulfill additional objectives while performing a given task. Many past studies showed that the redundancy may be used to optimize the performance index such as manipulability (Yoshikawa, 1985), energy efficiency (Santhakumar, 2013), and stability (Takanishi et al., 1989). The redundancy resolution was adopted to avoid the singularity (Mohan and Kim, 2012) and used to determine the task priority during execution of the underwater operations (Antonelli and Chiaverini, 1998). Furthermore, it was used to generate the desired trajectory so as to minimize the drag force and joint torques (Hollerbach and Suh, 1987). The joint trajectories were generated to minimize the restoring moments (Han et al., 2011). Also, redundancy resolution was used for fault-tolerant system (Soylu et al., 2010).

In this study, a new performance index based on zero moment point (ZMP) concept (Vukobratovic and Borovac, 2004; Choi, 2012) is proposed to improve the stability of the underwater vehicle in disturbance caused by the motion of the manipulator. ZMP generally specifies that the dynamic reaction force when the foot of the humanoid robot comes into contact with the ground does not cause any moment in the horizontal direction. Using the ZMP concept, this study introduces a method of stabilizing an underwater vehicle by moving the ZMP calculated by the mass and moment of inertia of the manipulator and object to the center of mass of the UVMS. In addition, a Redundancy Resolution method is proposed to generate an optimal trajectory of UVMS.

This paper is organized as follows. In Section 2, the kinematic and dynamic equations of the UVMS are introduced. In section 3, the redundancy resolution and ZMP algorithm are proposed. GPM is also presented to find optimal solution. Section 4 shows the simulation results of UVMS that follows the trajectories generated by redundancy resolution and ZMP algorithm.

Paper submitted 05/17/17; revised 12/05/17; accepted 12/08/17. Author for correspondence: Hyeung-Sik Choi (e-mail: hchoi@kmou.ac.kr).
[1] Ocean Science and Technology School, KIOST-KMOU, Busan, South Korea.
[2] Department of Mechanical Engineering, Korea Maritime and Ocean University, South Korea.

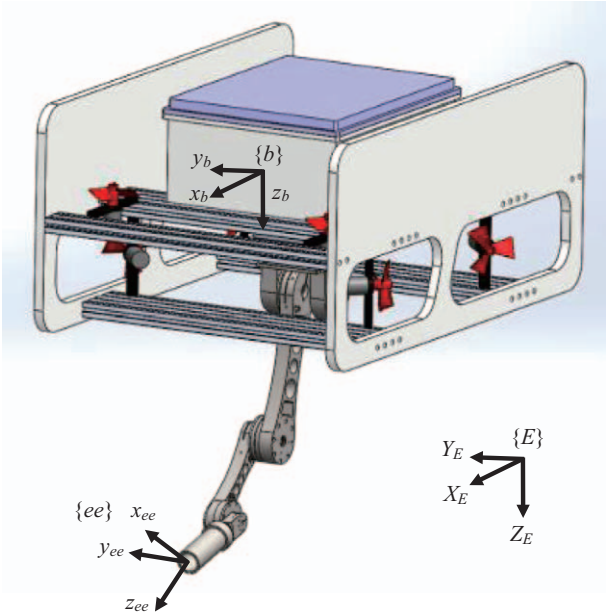

Fig. 1. Coordinate systems for the UVMS.

In Section 5, experiments are performed to verify the performance of the ZMP algorithm and redundancy resolution method.

II. MODELING OF THE UVMS

1. UVMS Kinematics

The coordinate system of an underwater vehicle with 3-DOF manipulator was illustrated in Fig. 1. $\{E\}$, $\{b\}$, and $\{ee\}$ represent the Earth-fixed frame, the body-fixed frame, and the end-effector frame, respectively.

The homogeneous transformation matrix from body-fixed frame to the inertial frame can be expressed as

$$ {}^{E}T_{b} = \begin{bmatrix} {}^{E}R_{b} & {}^{E}p_{b} \\ 0_{1\times 3} & 1 \end{bmatrix} \tag{1} $$

where ${}^{E}p_{b} \in \Re^{3\times 1}$ is the potion vector of underwater vehicle in terms of the Earth-fixed frame, and ${}^{E}R_{b} \in \Re^{3\times 3}$ is the rotation matrix of body-fixed frame with respect to the Earth-fixed frame. The position and orientation of the end-effector can be defined as

$$ {}^{b}T_{ee} = \begin{bmatrix} {}^{b}R_{ee} & {}^{b}p_{ee} \\ 0_{1\times 3} & 1 \end{bmatrix} \tag{2} $$

where ${}^{b}R_{ee}$, ${}^{b}p_{ee}$ can be calculated by the joint variable of the manipulator, ${}^{b}q_{i}$. By multiplying (1) and (2), the homogeneous transformation matrix from the Earth-fixed frame to the end-effector can be computed as

$$ {}^{E}T_{ee} = {}^{E}T_{b}\,{}^{b}T_{ee} = \begin{bmatrix} {}^{E}R_{ee} & {}^{E}p_{ee} \\ 0_{1\times 3} & 1 \end{bmatrix} \tag{3} $$

2. Dynamic Modeling of a UVMS

The dynamic modeling for an UVMS can be obtained by considering the coupled dynamics between the underwater vehicle and the manipulator (Dannigan, 1998). Hence, the dynamics equations of the whole system with respect to the body-fixed frame can be written in the form as (4) and (5)

$$ \mathbf{M}_{s}(\Theta)\dot{\xi} + \mathbf{C}_{s}(\Theta,\xi)\xi + \mathbf{D}_{s}(\Theta,\xi)\xi + G_{s}(\eta,\Theta) = \tau_{s} \tag{4} $$

where

$$ \xi = \left[v,\ \dot{\Theta}\right]^{T},\ M_{s} = \begin{bmatrix} M_{v} & 0 \\ 0 & M_{m}(\Theta) \end{bmatrix}, C_{s} = \begin{bmatrix} C_{v} & 0 \\ 0 & C_{m}(\Theta,\dot{\Theta}) \end{bmatrix}, $$
$$ D_{s} = \begin{bmatrix} D_{v}(v) & 0 \\ 0 & D_{m}(\Theta,\dot{\Theta}) \end{bmatrix}, G_{s} = \begin{bmatrix} G_{v}(\eta) \\ G_{m}(\Theta) \end{bmatrix}, \tau_{s} = \begin{bmatrix} \tau_{v} + \tau_{mv} \\ \tau_{m} \end{bmatrix} \tag{5} $$

ξ is the linear and angular velocity vector of the whole system in terms of body-fixed frame. M_s, C_s, D_s, and G_s are matrix for the mass and inertia, Coriolis and centripetal forces, hydrodynamic lift and damping forces, restoring forces and moments of the whole system, respectively. τ_s represents the control input for an underwater vehicle and a manipulator.

III. REDUNDANCY RESOLUTION

In general, trajectories of an underwater vehicle and an end-effector should be given to performing specified tasks in water. To track given trajectories in task space, trajectories of the underwater vehicle and the joint of manipulator can be obtained through inverse kinematic analysis in the joint space.

The redundant UVMS has various combinations of joint velocities that do not affect the given velocity profile of an end-effector and this could induce the self-motion of the vehicle. Hence, by using the degrees of redundancy, the desired trajectories of vehicle and joints can be determined without affecting its motion in the task space. The relation between the posture of an end-effector and the system configuration can be represented as shown in (6).

$$ {}^{b}\eta_{ee} = f(\Theta) \tag{6} $$

where ${}^{b}\eta_{ee} \in \Re^{6\times 1}$ is the vector including the position and orientation of an end-effector expressed with respect to the body-fixed frame; η and q are the position vector of an underwater vehicle and the joint angles vector respectively.

The following equation can be obtained by differentiating

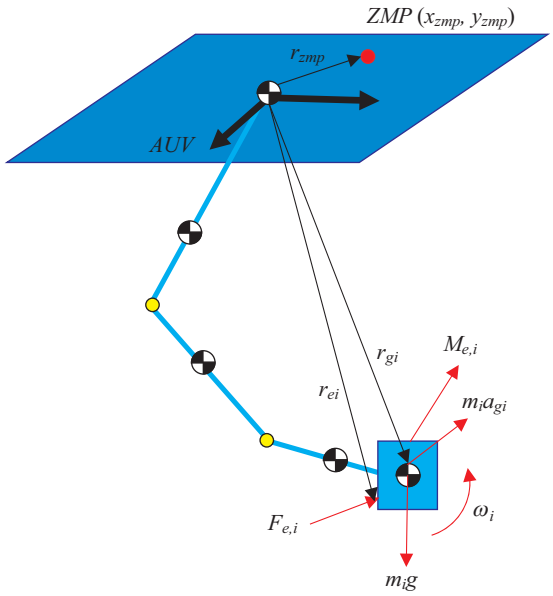

Fig. 2. A concept of ZMP for stabilization of an UVMS.

(6) with respect to time.

$$ {}^{b}\dot{\eta}_{ee} = \mathbf{J}(\Theta)\dot{\Theta} \tag{7}$$

where J is the Jacobian matrix and is a $6 \times (6+n)$ matrix in this work. n is the number of joints. When the velocity profile of an end-effector is given, the joint velocities of a manipulator and the velocity of an underwater vehicle can be determined by the redundancy resolution.

$$ \dot{\Theta} = \mathbf{J}(\Theta)^{\#} \cdot {}^{b}\dot{\eta}_{ee} + \left(\mathbf{I}_{3\times 3} - \mathbf{J}(\Theta)^{\#}\mathbf{J}(\Theta)\right)\gamma \tag{8}$$

where $J^{\#}$ is the Moore-Penrose pseudo-inverse matrix of the Jacobian matrix J and this can be calculated as according to (9)

$$ \mathbf{J}(\Theta)^{\#} = \mathbf{J}(\Theta)^{T}\left[\mathbf{J}(\Theta)\mathbf{J}(\Theta)^{T}\right]^{-1} \tag{9}$$

1. Performance indexes for Stabilization and Implementation of a UVMS

The Zero Moment Point(ZMP) is a point at which the sum of moments generated by all external forces and inertial forces including gravity acting on the rigid body becomes zero. In this works, the performance index is introduced based on the concept of ZMP which improves the dynamic stability of an UVMS.

As shown in Fig. 2, the moment equation that the ZMP with the sum of the moments of the system consisting of several link chains is zero can be expressed as follows(Kim, 2016).

$$\begin{aligned}\sum_i \left(r_{gi} - r_{zmp}\right)\times m_i g + \sum_i \left(r_{ei} - r_{zmp}\right)\times F_{ei} \\ + \sum_i M_{ei} - \sum_i \left(r_{gi} - r_{zmp}\right)\times m_i a_{gi} \\ - \sum_i \left[\mathbf{I}_i\dot{\omega}_i + \omega_i \times \left(\mathbf{I}_i\omega_i\right)\right] = 0\end{aligned} \tag{10}$$

where i is subscript that represents each link chain, and r_{zmp}, r_{gi} and r_{ei} represent the position vector from the origin to *ZMP* of coordinates system, the position vector to the mass center of the ith link, and the position vector to the point of application of external force on the ith link respectively. Also, g, m_i and a_{gi} represent gravitational acceleration vector, the mass of the ith link and mass-centered acceleration vector respectively, and $F_{e,i}$ and $M_{e,i}$ represent the force and moment acting on the ith link from outside respectively.

From Eq. (10), position of the ZMP can be obtained as

$$ x_{zmp} = \frac{\left\{\begin{array}{c}\sum_i m_i \ddot{x}_{gi} z_{gi} + \sum_i m_i (g - \ddot{z}_{gi}) x_{gi} + \sum_i (F_{ez,i} x_{ei} - F_{ez,i} z_{ei}) \\ + \sum_i \left[I_{yy,i}\dot{\omega}_{yi} + (I_{xx,i} - I_{zz,i})\omega_{xi}\omega_{zi}\right]\end{array}\right\}}{\sum_i \left(m_i g - m_i \ddot{z}_{gi} + F_{ez,i}\right)} \tag{11}$$

$$ y_{zmp} = \frac{\left\{\begin{array}{c}\sum_i m_i \ddot{y}_{gi} z_{gi} + \sum_i m_i (g - \ddot{z}_{gi}) y_{gi} + \sum_i (F_{ez,i} y_{ei} - F_{ey,i} z_{ei}) \\ - \sum_i \left[I_{xx,i}\dot{\omega}_{xi} + (I_{zz,i} - I_{yy,i})\omega_{zi}\omega_{yi}\right]\end{array}\right\}}{\sum_i \left(m_i g - m_i \ddot{z}_{gi} + F_{ez,i}\right)} \tag{12}$$

The ZMP concept can be used to create a trajectory that moves the center of gravity of the manipulator as close to the center of gravity of the underwater vehicle as possible while performing specified tasks.

The distance between the mass center position of the UVMS and the ZMP is set as the performance index as in (13). In this paper, the performance index is minimized in conjunction with a redundancy analysis.

$$ \Xi_1(\eta, \Theta) = \frac{1}{2}\mathbf{W}_{p1}\left\|r_{zmp} - \Delta_{zmp}\right\|^2 = \frac{1}{2}\mathbf{W}_{p1}(x_{zmp} - \Delta_x)^2 \tag{13}$$

where $\mathbf{W}_{p1}$ represents the weight matrix.

For an implementation of UVMS, a joint limitation is also taken as performance index for generation of manipulator motion as shown in (14)

$$\begin{aligned}\Xi_2(\Theta) &= \frac{1}{2}\sum_{i=1}^{3}\mathbf{W}_{p2}\left(\frac{\theta_i - \theta_{i,mid}}{\theta_{i,\mathrm{int}}}\right)^2 \\ \theta_{i,mid} &= \frac{\theta_{i,\max} + \theta_{i,\min}}{2}, \theta_{i,\mathrm{int}} = \frac{\theta_{i,\max} - \theta_{i,\min}}{2}\end{aligned} \tag{14}$$

Table 1. Parameters for the floater and manipulator.

Parameters		Values [unit]
Floater	L × H × W	1 × 0.2 × 0.3 [m^3]
	Mass	5 [kg]
Link 1	Length	0.3 [m]
	Mass	3 [kg]
Link 2	Length	0.2 [m]
	Mass	2 [kg]
Link 3	Length	0.18 [m]
	Mass	2 [kg]

where $\theta_{i,\max}$ and $\theta_{i,\min}$ represent maximum and minimum limit angle of the ith link respectively, and $\mathbf{W}_{p2}$ represents the weight matrix.

To satisfy both additional tasks, a performance index is proposed that manipulator joint angle trajectory can be created to improve the stability of the whole UVMS within the limited range of manipulator joint angle, which is expressed as

$$\Xi(\Theta)=\frac{1}{2}\mathbf{W}_{p1}(x_{zmp}-\Delta_x)^2+\frac{1}{2}\sum_{i=1}^{3}\mathbf{W}_{p2,i}\left(\frac{\theta_i-\theta_{i,mid}}{\theta_{i,\text{int}}}\right)^2 \tag{15}$$

2. Gradient Projection Method for Optimization

The first term in (8) is the particular solution, which is determined from the given velocity of an end-effector. The second term in (8) is the homogeneous solution, which is obtained by the projection onto the null-space of Jacobian matrix J. It represents the self-motion which does not affect the task motion. Hence, the vector γ can be defined in order to obtain the optimal solution for the specified performance index. The solution in null space can be obtained by conducting a redundancy analysis using the gradient projection method (GPM) (Calamai and Moré, 1987) for the proposed performance index as shown in (13).

$$\gamma=-\kappa\cdot\nabla\Xi;$$
$$\nabla\Xi=\left[\frac{\partial\Xi}{\partial\theta_1},\ \frac{\partial\Xi}{\partial\theta_2},\ \cdots,\ \frac{\partial\Xi}{\partial\theta_N}\right]^T \tag{16}$$

where κ and $\nabla\Xi$ represent a positive gradient constant and the gradient vector of performance index respectively.

IV. SIMULATION

To verify the performance of the joint trajectory generation using the proposed redundancy resolution (RR) algorithm, a simulation of testbed consisting of a floater with 3-DOF manipulator shown in Fig. 3 was performed and the proposed algorithm was applied to this platform. Table 1 shows the parameters for the testbed. For comparison with the RR algorithm, a simulation using pseudo inverse (PI) algorithm was performed under the same condition. Applying only PI using the first term in (8) to solve the inverse kinematics is described as follows.

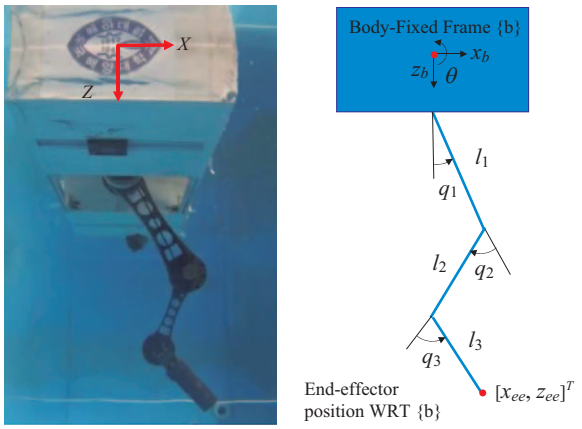

Fig. 3. Testbed composed of a floater with 3-DOF manipulator.

$$\dot{\Theta}=\mathbf{J}(\Theta)^{\#}\cdot{}^{b}\dot{\eta}_{ee} \tag{17}$$

For both cases, the end-effector is commanded to follow the line from the initial position (0 m, 0.55 m) to the final position (0.1 m, 0.55 m) in the X-Z plane for 6sec.

1. Generation of Trajectories of End-Effector

To carry out the redundancy resolution, trajectories of an end-effector in the task-space should be given. The trajectory with start and end velocities between two configurations is expressed using a polynomial function of time as follows (Spong, 2006).

$$q(t)=a_0+a_1t+a_2t^2+a_3t^3 \tag{18}$$

Then we can get desired velocity is given as

$$\dot{q}(t)=a_1t+2a_2t+3a_3t^2 \tag{19}$$

Through the equations (18) and (19), a matrix equation can be obtained as in (20).

$$\begin{bmatrix}1 & t_0 & t_0^2 & t_0^3\\ 0 & 1 & 2t_0 & 3t_0^2\\ 1 & t_f & t_f^2 & t_f^3\\ 0 & 1 & 2t_f & 3t_f^2\end{bmatrix}\begin{bmatrix}a_0\\ a_1\\ a_2\\ a_3\end{bmatrix}=\begin{bmatrix}q_0\\ v_0\\ q_f\\ v_f\end{bmatrix} \tag{20}$$

where t_0 and t_f represent start time and end time, $[a_0, a_1, a_2, a_3]^T$ is the coefficients of the cubic polynomial, and $[q_0, v_0, q_f, v_f]^T$ is the initial and final positions and velocities.

In this simulations, trajectories and velocities of the end-effector is given by using Eq. (20).

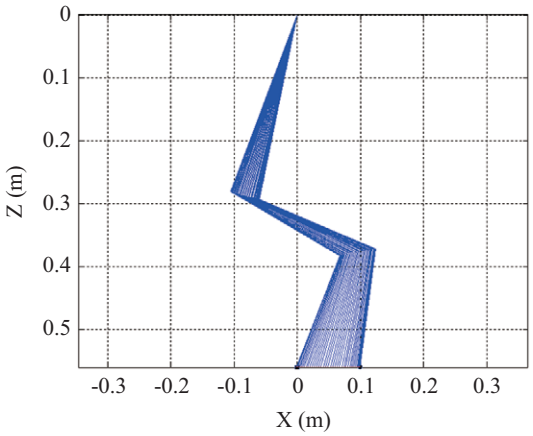

Fig. 4. Stick diagram of the testbed using only PI.

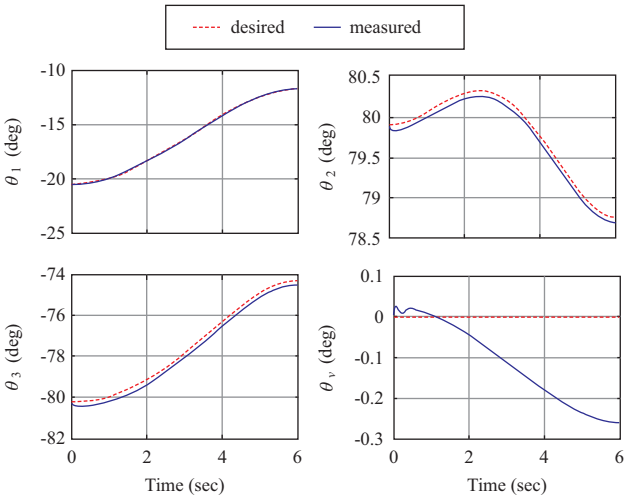

Fig. 5. Joint variables and pitch angle of testbed using only PI.

2. Trajectory Following Simulation

Fig. 4 shows the generated the joint angle trajectories of the manipulator using the only PI, without performing the RR. As can be seen from the results, the joints trajectories can be generated so that the end-effector of the manipulator follows the desired trajectory with only the PI. As shown in Fig. 5, the joint variables and the pitch angle of the testbed were generated by using PI. Fig. 6 indicates that the desired trajectory of end-effector was generated as a smooth curve using a time polynomial function.

On the other hand, Fig. 7 shows the result of the simulation through the RR to keep the ZMP position as close as possible to the center of mass of the underwater vehicle to improve the dynamic stability of the entire system. It is shown that extra DOFs of manipulator were assigned to secure the dynamic stability of system while performing a given task.

As shown in Fig. 8, RR was used to generate the joint variables and pitch angle of the test bed. Fig. 9 shows that the desired and measured trajectories of end-effector. Comparing Fig. 5 and

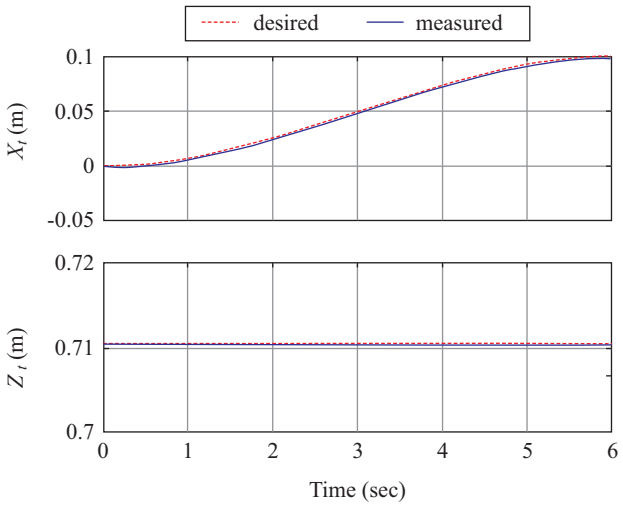

Fig. 6. Trajectories of end-effector using only PI.

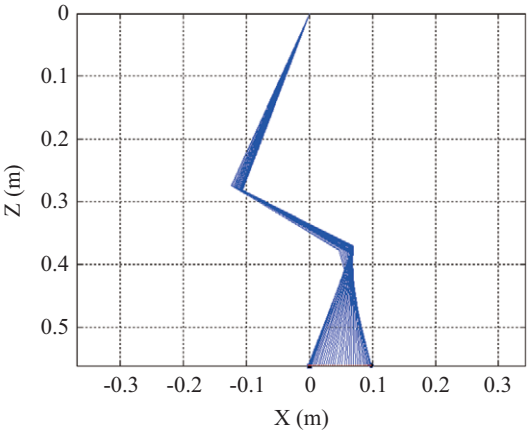

Fig. 7. Stick diagram of the testbed using proposed RR.

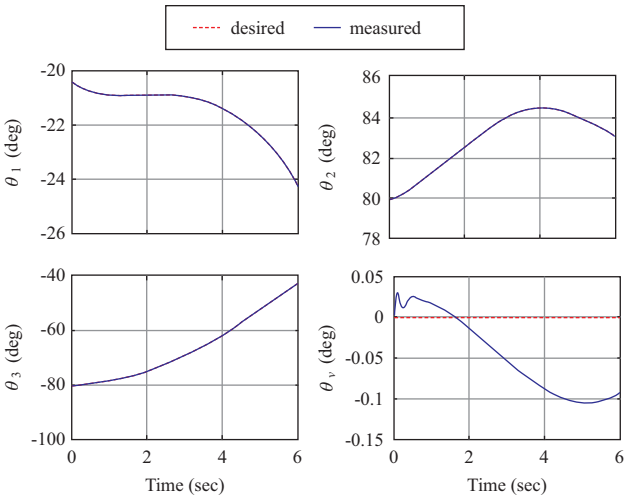

Fig. 8. Joint variables and pitch angle of testbed proposed RR.

Fig. 8, the starting positions of the joints of the PI and RR are the same, but the combination of the joints over time is different.

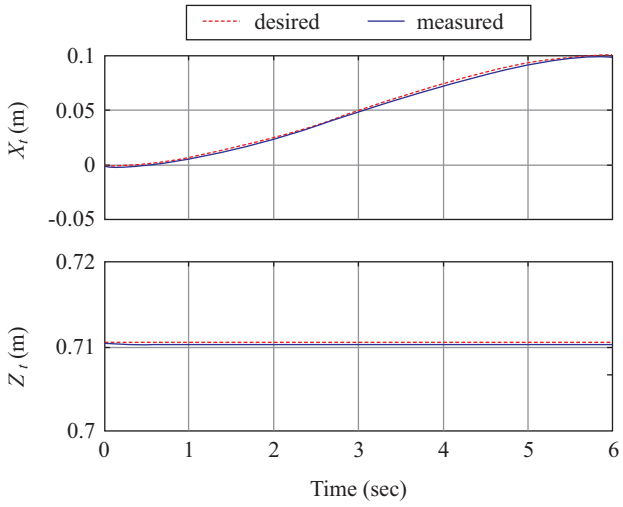

Fig. 9. Trajectories of end-effector using proposed RR.

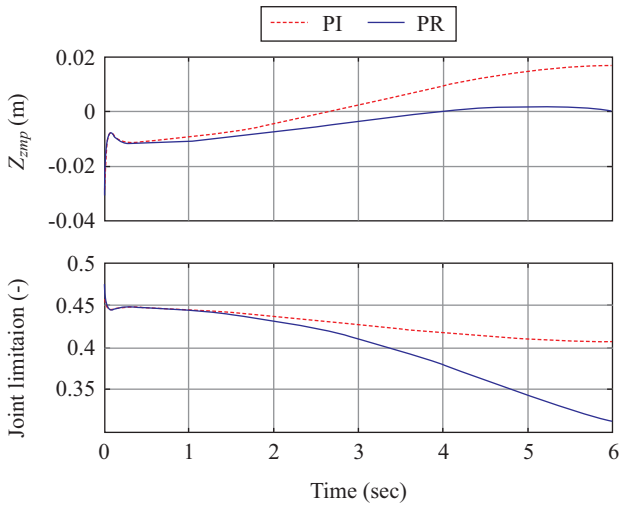

Fig. 10. Comparison of performance index between PI and RR.

As shown in Fig. 9, the RR algorithm follows the desired trajectory of the end-effector as well as PI.

Fig. 10 indicates the comparison of performance indices of the simulated results using PI and RR. It can be seen from the trajectory of x_{ZMP}, the RR keeps the dynamic stability by making the distance between center of gravity of the underwater vehicle and x_{ZMP} close to zero through self-motion. On the contrary, the x_{ZMP} of PI has passed zero after 3 seconds. The result shows that the ZMP of the whole system is located closer to the center of mass of the underwater vehicle through the RR. It can also be seen that by lowering the performance index of joint limitation, it creates a trajectory that does not go beyond the limits of the manipulator's joints.

V. EXPERIMENTS

1. Trajectory Following Control

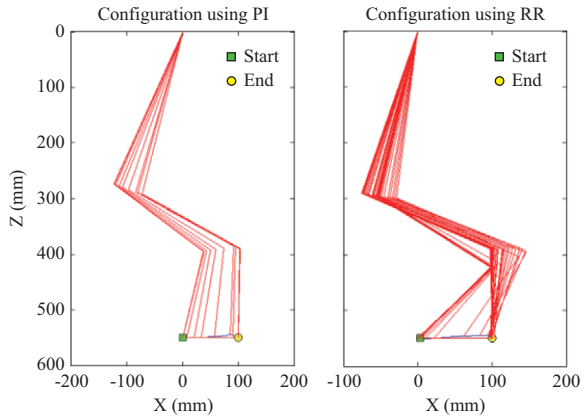

Fig. 11. Test results of configurations of manipulator using PI only and RR.

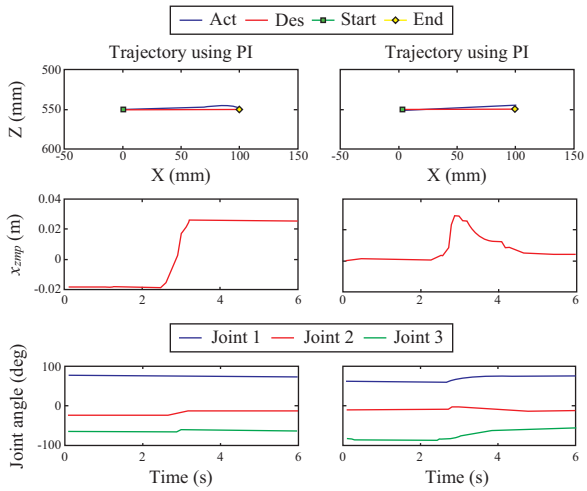

Fig. 12. Test results of trajectories using PI only and RR.

To evaluate trajectory following performance of the RR, an optimization for the proposed performance index as Eq. (15) was conducted. For comparison with the RR algorithm, a pseudo inverse (PI) algorithm was also applied to the testbed with the same initial conditions and desired trajectory. For both cases, the end-effector is commanded to follow a line from the initial position (0 mm, 550 mm) to the destination position (100 mm, 550 mm) in the X-Z plane. This command excites the stability of the manipulator attached at the floating vehicle. Since the excitation generates the pitching motion of the system, the mass center of the whole system should be controlled to move the mass center position.

Under these conditions, the RR and PI were applied to the testbed as shown in Fig. 3. Fig. 11 shows configurations of manipulator trajectory using PI and RR in X-Z axis. In the case of using RR, each joint changes the joint angle to reduce the x_{ZMP} with keeping the end-effector position. In Eq. (15), stability and mobility of the UVMS can be improved through tuning the $\mathbf{W}_{p1}$ and $\mathbf{W}_{p2}$ as weight matrix.

According to the test results, Fig. 12 indicates that both al-

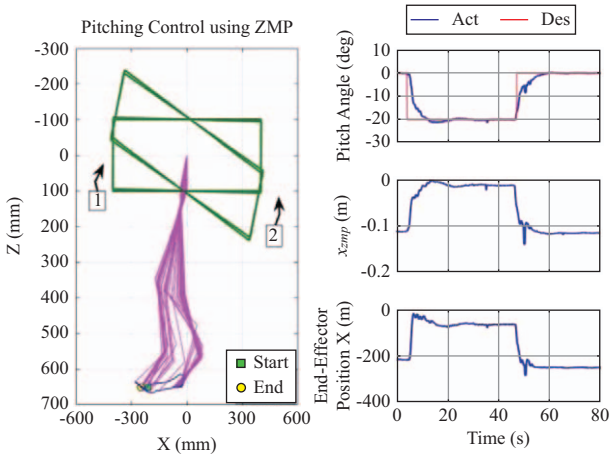

Fig. 13. Control pitch angle of a testbed using ZMP.

gorithms generate similar and acceptable tracking errors in the PI and RR cases with 5 mm position error in Z axis. And the second line in Fig. 12 represents the distance between the mass center position of the whole system and the x_{ZMP}. If x_{ZMP} approaches to zero distance, the whole system goes to the stable state. So, the plot shows that application of the PI case does not decrease x_{ZMP} during following the desired trajectory. On the other hand, the RR makes x_{ZMP} decrease monotonically. This is similar to the simulation results presented above.

The merit of the RR is that the manipulator can reduce the restoring moment by minimizing the distance between ZMP X-axis and the mass center of the whole system while tracking the trajectory.

2. Pitching Control Using ZMP

Using the redundancy of the manipulator, additional joint angles can be confined along the desired ones while using the ZMP algorithm which compensates the forces and moments caused by the motion of the manipulator. In this experiment, while applying the ZMP algorithm, pitch angle of the floating vehicle was controlled with keeping the depth of the end-effector by changing of x_{ZMP} and end-effector position in X-axis. According to these constraints and ZMP algorithm, experiments were conducted, and results are presented in Fig. 13. The red line and blue line represents the desired and actual pitch angle of the floating vehicle in the top of the right-hand side, the middle one represents the x_{ZMP}, and the bottom one is the end-effector position in X-axis. Also, the left hand side figure represents the results of the orientation of the floating vehicle when the pitching control was applied using ZMP algorithm. As shown in Fig. 13, the experiments were carried out in two steps. In the first step, the pitch angle of the floating vehicle was controlled to move from 0° to -20° and kept at -20° by changing x_{ZMP} from -110 mm to -10 mm and end-effector position from -210 mm to -60 mm. After the floating vehicle was stable at time 20 sec, the second command was issued to return the pitch angle from -20° to 0° at time 48 sec. In order to restore initial pitch angle of the floating vehicle as 0°, x_{ZMP} and end-effector in X-axis were replaced to the each initial value as -110 mm and -210 mm respectively. During the two steps, end-effector was controlled to keep at 650 mm in Z axis using the optimal algorithm.

This results show that the ZMP and the center of gravity distance of the underwater vehicle can be adjusted to help maintain the specific posture of the underwater vehicle. This means that it is possible to reduce the thrust force required to maintain a stable posture of the underwater vehicle.

VI. CONCLUSION

In this paper, the dynamics modeling was conducted considering the coupled dynamics of the redundant system composed of the vehicle and the manipulator. To improve the stability of the vehicle due to manipulator motion, the ZMP algorithm was proposed. The performance index was defined and the redundancy resolution (RR) algorithm was proposed to minimize the restoring moment of the whole system including a payload to enhance the motion stability and to satisfy the joint constraints of the manipulator.

To validate the proposed ZMP algorithm and RR algorithm, an UVMS testbed composed of a floating body with 3 DOF manipulator was constructed. Experiments of trajectory tracking were performed to evaluate the performance of the RR algorithm with the ZMP algorithm, and the results were compared with that of the PI algorithm under the same conditions.

The results show that the RR algorithm with ZMP shows good performance in the stable posture of the whole system and in trajectory tracking of the manipulator. Also, in comparison with the PI algorithm, it shows better performance in motion stability and trajectory tracking.

ACKNOWLEDGMENT

This research is a part of the project National Research Foundation of Korea (NRF 2016R1A2B4011875) and supported by Basic Science Research Program through the National Research Foundation of Korea (NRF) funded by the Ministry of Education (2015R1D1A3A01015804).

REFERENCES

Antonelli, G. and S. Chiaverini (1998). Task-priority redundancy resolution for underwater vehicle-manipulator systems. In Robotics and Automation, 1998. Proceedings. 1998 IEEE International Conference 1, 768-773.

Calamai, P. H. and J. J. Moré (1987). Projected gradient methods for linearly constrained problems. Mathematical programming 39(1), 93-116.

Choi, D. I. and J. H. Oh (2012). ZMP stabilization of rapid mobile manipulator. in Proceedings IEEE International Conference on Robotics and Automation, 883-888.

Dannigan, M. W. and G. T. Russell (1998). Evaluation and reduction of the dynamic coupling between a manipulator and an underwater vehicle. IEEE Journal of Oceanic Engineering 23(3), 260-273.

Han, J. H., J. H. Park and W. K. Chung (2011). Robust coordinated motion control of an underwater vehicle-manipulator system with minimizing restor-

ing moments. Journal of Ocean Engineering 38(10), 1197-1206.
Hollerbach, J. and K. Suh (1987). Redundancy resolution of manipulators through torque optimization. IEEE Journal on Robotics and Automation 3(4), 308-316.
Kim, D. H. (2016). Redundancy Resolution and Robust Controller Design for Dynamic Stability Enhancement of Underwater Vehicle-Manipulator Systems. Ph.D Dissertation, Busan, Korea Maritime and Ocean University. (in Korean).
Mohan, S. and J. Kim (2012). Indirect adaptive control of an autonomous underwater vehicle-manipulator system for underwater manipulation tasks. Ocean Engineering 54, 233-243.
Santhakumar, M. (2013). Task space trajectory tracking control of an underwater vehicle-manipulator system under ocean currents.
Soylu, S., B. J. Buckham and R. P. Podhorodeski (2010). Redundancy resolution for underwater mobile manipulators. Ocean Engineering 37(2), 325-343.
Spong, M. W., S. Hutchinson and M. Vidyasagar (2006). Robot Modeling and Control (Vol. 3). New York: Wiley.
Takanishi, A., M. Tochizawa, H. Karaki and I. Kato (1989). Dynamic biped walking stabilized with optimal trunk and waist motion. in Proceedings IEEE International Workshop on Intelligent Robots and Systems, 187-192.
Vukobratović, M. and B. Borovac (2004). Zero-moment point-thirty five years of its life. International journal of humanoid robotics 1(01), 157-173.
Yoshikawa, T. (1985). Manipulability and redundancy control of robotic mechanisms. in Proceedings IEEE International Conference on Robotics and Automation, 1004-1009.